Fast surface reconstruction and hole filling using positive definite Radial Basis Functions

G. Casciola [a], D.Lazzaro [a], L.B.Montefusco [a], S.Morigi [a]

[a] *Department of Mathematics, University of Bologna, P.zza di Porta San Donato 5, 40127 Bologna, Italy*

Surface reconstruction from large unorganized data sets is very challenging, especially if the data present undesired holes. This is usually the case when the data come from laser scanner 3D acquisitions or if they represent damaged objects to be restored. An attractive field of research focuses on situations in which these holes are too geometrically and topologically complex to fill using triangulation algorithms.

In this work a local approach to surface reconstruction from point-clouds based on positive definite Radial Basis Functions (RBF) is presented that progressively fills the holes by expanding the neighbouring information. The method is based on the algorithm introduced in [7] which has been successfully tested for the smooth multivariate interpolation of large scattered data sets. The local nature of the algorithm allows for real time handling of large amounts of data, since the computation is limited to suitable small areas, thus avoiding the critical efficiency problem involved in RBF multivariate interpolation. Several tests on simulated and real data sets demonstrate the efficiency and the quality of the reconstructions obtained using the proposed algorithm.

Keywords: radial basis function, surface reconstruction, local interpolation, hole filling
AMS subject classification: 65D17, 65D05, 65Y20.

1 Introduction

The digitalization and reconstruction of 3D shapes has numerous applications in areas that include manufacturing, virtual simulation, medicine, entertainment, consumer marketing and archaeology. Methods to digitize and reconstruct the shapes of complex objects have evolved rapidly in recent years. The speed and accuracy of digitizing technologies allows us to take detailed measurements of the objects, but in order to capture the complete shape of an object, many thousands of samples must be acquired. The resulting mass of data requires algorithms that can efficiently and reliably generate computer models from these samples.

The reconstruction of a 3D model is usually obtained from scattered data points sampled from the surface of the physical 3D object. The acquisition of the data is realized through 3D scanning systems which are able to capture a dense and accurate sampling usually organized into *range images*, i.e. sets of distances from the sensor to the object being scanned. Each range image needs to be filtered to remove artifacts and noise, and to fill the holes. Using laser light scanners, in fact, gives rise to range images which can be noisy and affected by artifacts, depending on their material and on the presence of partially reflecting surfaces. Moreover, they can present simple or topologically complex holes. Most of them can be naturally filled by the overlapping range images process, since the most fundamental cause of holes is occlusion - recesses too deep to be observed using a particular angle.

Email addresses: casciola@dm.unibo.it (G. Casciola), lazzaro@csr.unibo.it (D.Lazzaro), montelau@dm.unibo.it (L.B.Montefusco), morigi@dm.unibo.it (S.Morigi).

However, holes can also be caused by low reflectance, constraints on scanner placement, or simply missing views. This is frequently observed in the scanning of works of art, which have a lot of self-occlusions and details. Works of art also impose significant restrictions on the scanner placement. Moreover, the holes can correspond to missing or damaged parts of the object when the scanning process is used, e.g. , in a computer aided restoration session.
Surface reconstruction from dense range data has been an active area of research for several years. The strategies have proceeded along two basic directions: reconstruction from unorganized points, and reconstruction that preserves the underlying structure of the acquired data. These two strategies can be further subdivided, according to whether they operate by reconstructing piecewise linear or smoother surfaces, or by reconstructing an implicit function. Examples of implicit surface reconstruction include the method of Hoppe [6], Bajaj [1] and, more recently, Beatson et al. [2], which use RBF to fit a signed distance function followed by an isosurface extraction.
Most of these approaches are not particularly concerned with the hole filling problem. In fact, they lead to a natural filling of the holes, which works well for simple holes in nearly flat surfaces, but not for convoluted geometric holes. In many applications it is important to be able to reconstruct this missing information for post-processing, as well as for presentation in a more plausible way. One widely used approach to hole filling consists in triangulating each connected component of the surface boundary, thereby filling the holes with a patch. Recently, in the pioneering work [3], the authors specifically address situations in which the holes are too topologically complex to fill using triangulation algorithms, and they propose solving the hole filling problem via isotropic diffusion of volumetric data (i.e., iterative Gaussian convolution of some distance function to the known data). The approach proposed by these authors produces watertight digital models, but it does not seem to give intuitive answers to the hole filling tests presented. We refer to this paper for an excellent and detailed description of the nature of the holes in scanning statues, and for a review of the literature on this subject.
In this work we consider a method which is designed for multivariate interpolation (approximation) of general data sets. It is based on an algorithm presented in an earlier paper [7] which makes local use of radial basis function interpolants. This local approach allows for real time handling of large amounts of data, since the computation is limited to suitable small areas, thus avoiding the critical efficiency problem involved in RBF multivariate interpolation (see e.g. [10] and references herein). Here we adapt the algorithm to the specific application of surface reconstruction from 3D scanning range data by including an efficient hole filling procedure, which progressively fills the holes by expanding the neighbouring information. The locality of the proposed method allows us to fill in a selected way only desiderated areas, without forcing a convex watertight model which can be obtained using a unique interpolant function.
The paper is organized as follows. In Section 2 we discuss some theoretical results on interpolation with RBF, which will be assumptions to derive a fast and robust local reconstruction method given in Section 3. In Section 4, we present the new hole filling method and we discuss some relating theoretical aspetcs. The corresponding algorithm, integrated in the reconstruction procedure, is described in Section 5. Results follow in Section 6, where the efficiency and the capabilities of our approach are demonstrated by considering real data sets.

2 Interpolation with positive definite Radial Basis Functions

The interpolation problem can be stated as follows. Given a set of distinct nodes $X = \{\mathbf{x}_i\}_{i=1}^N \subset \Omega \subset \mathbb{R}^d$, and a set of function values $\Im = \{f_i\}_{i=1}^N \subset \mathbb{R}$, the radial basis

function interpolant $s : \mathbb{R}^d \to \mathbb{R}$ on X is given by:

$$s(\mathbf{x}) = \sum_{j=1}^{N} c_j \varphi(\|\mathbf{x} - \mathbf{x}_j\|_2), \tag{1}$$

where the function $\varphi : [0, \infty) \to \mathbb{R}$ is called *radial basis function*, and the points $\mathbf{x}_j$ are referred to as *centers* of the radial basis functions. The coefficients $c_1, c_2, \ldots, c_N$ are determined by the interpolation conditions

$$s(\mathbf{x}_i) = f_i, \quad i = 1, .., N \tag{2}$$

which lead to the linear system

$$A_{X,\varphi}\mathbf{c} = \mathbf{f} \tag{3}$$

with $A_{X,\varphi} = (\varphi(\|\mathbf{x}_i - \mathbf{x}_j\|_2))_{1 \le i,j \le N}$. In order that the system (3) be solvable, the interpolation matrix $A_{X,\varphi}$ must be non-singular. In this work, we require that the matrix $A_{X,\varphi}$ is positive definite. In this case, following, e.g., the definition in [12], the function $\varphi(\|\cdot\|)$ is said to be positive definite in $\mathbb{R}^d$, which we abbreviate by $\varphi(\|\cdot\|) \in PD_d$.
Well known PD_d radial basis functions are the inverse multiquadrics. However, in this case, the interpolation matrix in (3) is non-sparse, and even modestly large data sets can lead to very ill-conditioned linear systems. Furthermore, the evaluation of the interpolant function (1) can become computationally expensive. In order to overcome these problems, Wendland [14] and Whu [13] have proposed compactly supported radial basis functions, which are positive definite on $\mathbb{R}^d$ according to their given order of smoothness. Although they represent an effort in the direction of localization, they still suffer from the inherent inability of the radial basis functions to interpolate very large data sets in a numerically stable and accurate way. In fact, the reconstruction may be poor, since it strongly depends on the radius of the support of these functions, which has to be scaled to adapt it to the different densities of the scattered data set. Moreover, improving the smoothness of φ improves the reproduction quality but, at the same time, also blows up the condition of $A_{X,\varphi}$.
For the purpose of this work, we considered inverse multiquadrics and compactly supported Wendland's functions, thus in the following we investigate the critical aspects of stability and accuracy for these classes of functions in greater details. For this aim, we first introduce the following two measures which characterize the density of the data set X: the *separation distance* q_X, which measures the closest pair of points in X, and the *fill distance* h_X, which represents the radius of the largest inner empty sphere, given by:

$$q_X = \frac{1}{2} \min_{1 \le i < j \le N} \|\mathbf{x}_i - \mathbf{x}_j\|_2, \qquad h_X = \sup_{\mathbf{x} \in \Omega} \min_{1 \le i \le N} \|\mathbf{x} - \mathbf{x}_i\|_2.$$

If we denote by $q_X(\mathbf{x})$ and $h_X(\mathbf{x})$ the previous quantities relative to the set $X \cup \{\mathbf{x}\}$, for each $\mathbf{x} \in \Omega$, we get the following relation:

$$q_X(\mathbf{x}) \le \min_{1 \le j \le N} \|\mathbf{x} - \mathbf{x}_j\|_2 \le h(\mathbf{x}).$$

The measures $q_X(\mathbf{x})$ and $h_X(\mathbf{x})$ are critical to the study of stability and accuracy of radial basis function interpolants. Concerning the conditions for the numerical stability of system (3), these can easily be derived from standard theory of numerical stability. In fact, the sensitivity of the solution $\mathbf{c}$ with respect to variations in the data is given by the condition number, which, in our case of symmetric positive definitive matrix, is given by the ratio $\frac{\Lambda}{\lambda}$

between the biggest and the smallest matrix eigenvalue.
Thus the stability analysis consists in finding good bounds for Λ and λ. In particular, it is necessary to find lower bounds on λ that are as tight as possible. This depends on the separation distance of the set X.
On the other hand, if the data are values of a function f belonging to a function space $\mathtt{F}$, the accuracy of the reconstruction is evaluated by the error of the interpolant defined by the solution of (3) with $f_i = f(\mathbf{x}_i)$. When $\mathtt{F}$ is defined via φ itself in a natural way [11], its characteristics depend on the d-variate generalized Fourier transform ϕ of φ. If ϕ decays at least algebraically at infinity, then $\mathtt{F}$ contains a certain Sobolev space, if ϕ decays exponentially, then $\mathtt{F}$ consists of C^∞ functions. In any case, the space $\mathtt{F}$ carries a specific seminorm $|\cdot|_{\mathtt{F}}$ and the interpolation error can be bounded by

$$|f(\mathbf{x}) - s(\mathbf{x})| \leq |f|_{\mathtt{F}} \cdot P(\mathbf{x}), \tag{4}$$

where the power function $P(\mathbf{x})$ is the norm of the error functional on $\mathtt{F}$, evaluated at $\mathbf{x}$. Note that P depends on $\mathbf{x}, X, \varphi$, and $\mathtt{F}$, but not on f.
Theoretical and numerical results have revealed a strict connection between the error and the sensitivity described by $P(\mathbf{x})$ and λ, respectively. Schaback proved in [11] that the accuracy and the condition number of the interpolation matrix cannot both be kept small. This effect is a sort of *uncertainty principle*, and it takes the form

$$P^2(\mathbf{x}) \geq \lambda(\mathbf{x}), \tag{5}$$

where $\lambda(\mathbf{x})$ is the smallest eigenvalue of the matrix $A_{X\cup\{\mathbf{x}\},\varphi}$.
Let us recall some well known results for a better comprehension of the choices we made in the design of our RBF interpolation method. According to [11] the known upper and lower bounds for $P(\mathbf{x})$ and $\lambda(\mathbf{x})$ take the forms

$$P(\mathbf{x})^2 \leq \mathcal{F}(h_X(\mathbf{x})) \quad \text{and} \quad \lambda(\mathbf{x}) \geq \mathcal{G}(q_X(\mathbf{x})), \text{respectively} \tag{6}$$

where $\mathcal{F}, \mathcal{G} : \mathbb{R}^+ \to \mathbb{R}^+$ are continuous and decreasing functions for small arguments. We refer to [11] for a list of known examples of functions $\mathcal{F}$ and $\mathcal{G}$ related to some special RBF. Considering the uncertainty principle (5), we then obtain the two-sided bounds

$$\mathcal{G}(q_X(\mathbf{x})) \leq \lambda(\mathbf{x}) \leq P^2(\mathbf{x}) \leq \mathcal{F}(h_X(\mathbf{x})). \tag{7}$$

These bounds can be made more useful for practical applications if conditions can be given under which $h_X(\mathbf{x})$ can be bounded from above, in terms of $q_X(\mathbf{x})$. This is the case if we deal with a set of centers $X \subset \Omega$ which is *quasi-uniform*, i.e. if there are $\rho > 0$ and $h > 0$, such that

$$\begin{aligned} &1.\ h_X(\mathbf{x}) \leq h \\ &2.\ q_X = \tfrac{1}{2}\min_{1\leq i<j\leq N} \|\mathbf{x}_i - \mathbf{x}_j\|_2 \geq h \cdot \rho. \end{aligned} \tag{8}$$

In this case we call h the *density* and ρ the *uniformity* of X with respect to Ω. For example, a regular square grid has uniformity $\rho = 1/\sqrt{2}$, while a triangular grid has $\rho = \sqrt{3}/3$ [4]. As proved in [11], for quasi-uniform sets of centers with density h and quasi-uniformity ρ, we have two-sided bounds

$$\mathcal{G}(h\epsilon) \leq \lambda(\mathbf{x}) \leq P^2(\mathbf{x}) \leq \mathcal{F}(h) \tag{9}$$

for all $\mathbf{x} \in \Omega$ with $q(\mathbf{x}) \geq h\epsilon$, and $\mathcal{G}(h) \leq \mathcal{F}(h\sqrt{d})$ for sufficiently small arguments. For inverse multiquadrics (with constant γ) these bounds decay exponentially, as we have $\mathcal{F}(h) = O(e^{-\rho/h})$, and $\mathcal{G}(h) = O(h^{-1}e^{-\gamma d/h})$ [8]. For compactly supported radial basis functions $\varphi \in PD_d \cap C^{2k}$ of minimal degree, the results from [12] state that $\mathcal{G}(h) = O(q_X^{-d-2k-1})$, and $\mathcal{F}(h) = O(h^{k+1/2})$. Thus the condition number of the interpolation matrix only grows polynomially, in terms of the separation distance, if the latter tends to zero.
The previous analysis highlights that, when we interpolate on a set of centers, the best possible situation for balancing the stability and the approximation behaviour is when the uniformity of the set is maximized. This suggests a criterion for selecting suitable subsets of X, on which a good compromise between stability and accuracy can be achieved. This is, in fact, the main feature of the proposed RBF interpolation method, which performs local interpolations on well selected quasi-uniform subsets of X, and obtains a global reconstruction by suitably weighting the local contributions.

3 The local approach to the reconstruction

In this section we describe a local method which is designed for the reconstruction of large general data sets. The reconstruction method is based on a technique presented in an earlier paper [7], that is here adapted to the construction of a digital surface model from range data acquired from a physical object.
Our local approach to the reconstruction exploits the characteristics of flexibility and accuracy which have made the radial basis functions a well established tool for multivariate interpolation, overcoming the drawbacks presented by RBF global interpolation methods, such as instability and unacceptable computational cost. The method is a variant of the well known modified Shepard's method proposed by Renka [9], and uses RBF interpolants as nodal functions.
We consider the set $X \subset \Omega \subset \mathbb{R}^d$, where, for convenience, Ω is assumed to be the convex hull of X, and the corresponding set of function values $\Im = \{f_i\}_{i=1,\cdots,N}$.
For each $\mathbf{x}_k \in X,\ k = 1, \cdots, N$, we associate a set $X_k = \{\mathbf{x}_i \in X, i \in I_k\}$, where I_k is the set of indexes of $N_q - 1$ *suitable* neighbours of $\mathbf{x}_k$, as well as $\mathbf{x}_k$ itself, and we determine an RBF *nodal function* $R_k(\mathbf{x})$ in the form:

$$R_k(\mathbf{x}) = \sum_{i \in I_k} c_i \varphi(\|\mathbf{x} - \mathbf{x}_i\|_2), \tag{10}$$

by solving on X_k the local interpolation problem:

$$R_k(\mathbf{x}_i) = f_i,\ i \in I_k.$$

In order to achieve a real local approach, it is necessary to limit the influence of $R_k(\mathbf{x})$ by means of a weight function which decreases with the inverse of the distance from $\mathbf{x}_k$. To further control the locality of the reconstruction, Renka in [9], has suggested to associate with each $\mathbf{x}_k$ a parameter r_{W_k}, named *radius of influence*, that truncates the contribution of the k-th nodal function outside of the circle with this radius. To choose the radius of influence r_{W_k}, a certain number N_W of points closed to $\mathbf{x}_k$ is considered, then r_{W_k} is taken as the distance from the farthest of these N_W points. $N_W (\geq N_q)$ is thus a parameter which has to be small enough to guarantee the locality of the method.

Therefore, we define, for each $\mathbf{x}_k$, the k-th nodal weight function as

$$\overline{W_k}(\mathbf{x}) = \frac{W_k(\mathbf{x})}{\sum_{i=1}^{N} W_i(\mathbf{x})}, \quad W_k(\mathbf{x}) = \left[\frac{(r_{W_k} - r_k(\mathbf{x}))_+}{r_{W_k} r_k(\mathbf{x})}\right]^p, \tag{11}$$

where $r_k(\mathbf{x}) = \|\mathbf{x} - \mathbf{x}_k\|_2$ and r_{W_k} is the radius of influence around the point $\mathbf{x}_k$. Thus the value f_k at $\mathbf{x}_k$ influences only the evaluation of points within this radius. It can be shown (see [5]) that the positive weights $\overline{W_k}(\mathbf{x})$ satisfy the cardinality relations $\overline{W_k}(\mathbf{x}_i) = \delta_{ik}, i, k = 1, ..., N$ and constitute a partition of unity, namely $\sum_{k=1}^{N} \overline{W_k}(\mathbf{x}) = 1$.

Finally, for each evaluation point $\mathbf{x}$, the reconstruction is obtained by a weighted combination of a few local contributions, namely the nodal functions whose radius of influence contains $\mathbf{x}$. More precisely,

$$F(\mathbf{x}) = \sum_{k \in N_{\mathbf{x}}} \overline{W_k}(\mathbf{x}) R_k(\mathbf{x}). \tag{12}$$

where $N_{\mathbf{x}}$ is the set of indexes of all the nodes $\mathbf{x}_k$ s.t. $\|\mathbf{x} - \mathbf{x}_k\|_2 < r_{W_k}$.
Note that the choice of the radial function $\varphi(\|\cdot\|) \in C^\ell(\mathbb{R}^d)$ leads to $F \in C^s(\Omega)$, where $s = \min\{p, \ell\}$. Moreover, for each $\mathbf{x} \in \Omega$, the global approximation error $E(\mathbf{x})$ is given by:

$$E(\mathbf{x}) = |f(\mathbf{x}) - F(\mathbf{x})| \leq \sum_{k=1}^{N} \overline{W_k}(\mathbf{x}) e_k(\mathbf{x}), \tag{13}$$

$e_k(\mathbf{x})$ being the interpolation error (4) of the RBF interpolant $R_k(\mathbf{x})$ on the set X_k. The choice of the sets X_k is therefore crucial for the effectiveness of the reconstruction algorithm and must be made with great care. In fact, as we are interested in the reconstruction of dense range data, a naive choice for X_k, given considering $\mathbf{x}_k$ and its nearest neighbours, would certainly lead to instability problems. According to the theoretical results of the previous section, we have therefore made a better choice obtained by selecting suitable neighbours of $\mathbf{x}_k$, such that the set X_k consists of quasi equi-spread points, thus satisfying the quasi-uniformity conditions (8). This strategy yields an interpolation matrix $A_{X_k,\varphi}$ with minimum condition number still maintaining a good approximation behaviour. Moreover, since each point $\mathbf{x}_j \in X$ is associated with a nodal function $R_j(\mathbf{x})$, the points discarded in the choice of X_k also give a contribution to the final reconstruction, thus avoiding any loss of information.
In the case of noisy data, or data which are affected by considerable acquisition errors, a local RBF least squares approximation is a better choice for the nodal function $R_k(\mathbf{x})$. For this aim, we select a subset $S_k \subset X_k$ of N_c points, including $\mathbf{x}_k$ itself, which represents the centers of the radial basis functions considered. Given $S_k = \{\mathbf{x}_j \in X_k; j \in J_k\}$, we consider the matrix $B_{X_k,\varphi} = (\varphi(\|\mathbf{x}_i - \mathbf{x}_j\|_2))_{i \in I_k, j \in J_k}$, and we solve the following minimization problem

$$\min_{\mathbf{c}} \|B_{X_k,\varphi}\mathbf{c} - \mathbf{f}_k\|_2, \tag{14}$$

where $\mathbf{f}_k$ is the vector of the function values $\{f_i\}, i \in I_k$, and the entries of $\mathbf{c}$ are the coefficients of the RBF approximant:

$$R_k(\mathbf{x}) = \sum_{j \in J_k} c_j \varphi(\|\mathbf{x} - \mathbf{x}_j\|_2), \tag{15}$$

Note that the choice of the centers guarantees that the matrix $B_{X_k,\varphi}$ is full rank, as its columns are in the column space of $A_{X_k,\varphi}$.

4 The hole filling method

The reconstruction method described in the previous section, for its local nature, preserves the topology of the data sets, that is, roughly speaking, any hole in the data set produces an hole in the reconstruction. This can be considered an advantage both when the original shape presents some empty regions, (think for example to eye holes in a carnival mask), and when it is necessary to preserve missing regions in an ancient sculpture. But, if we are in the case of lacunary data that we want to restore, the local approach just described can be easily expanded with an efficient method for filling these holes. This will be the subject of the current section.
We now deal with the problem of the reconstruction of an RBF function on a data set $(X, \Im)$ which presents an empty, lacunary or damaged region. Let us call this region for simplicity *the hole*. The reconstruction method exploits only the available information on the hole surroundings that we denote by $B \subset X$, thus the processing is limited to the vicinities of the hole. The simplest approach we can consider, is a global reconstruction on B using relation (1); this would lead us to two main drawbacks. First, the gap in the data domain would produce a fill distance parameter h_B large with respect to q_B, thus losing the quasi uniformity conditions. This would give rise to the well known problems regarding accuracy and stability in the reconstruction. Moreover, the global method would fill the gap without allowing any kind of control on the shape of the reconstructed region.
From the above considerations, we propose a *multilayer technique* which incrementally expands the information on the hole boundary until the gap has been completely filled. This approach reaches the following goals: it maintains the quasi-uniformity conditions for each local interpolant, and enables a local control on the reconstruction by suitably setting the local nodal function parameters.
The key idea of the multilayer method is the following. We build a uniform grid, with an estimated grid data density H_G, and we overlap it on the boundary data B, thus filling completely the missing part in the data domain X. This set of grid points is denoted by G. In order to incrementally extend the original data set $(X, \Im)$ for including the new set $(G, \Im_G)$, we proceed with a decomposition of $B \cup G$ into a nested sequence of layers:

$$B = L_0 \subset L_1 \subset L_2 \subset \cdots L_{NL} \equiv B \cup G,$$

according to the hole width and to the grid data density. This layer structure, shown in Fig.1, allows us to fill the hole by splitting up the reconstruction into NL steps. Each step m, for $m = 1, \ldots, NL$, consists of the following three phases.

- First we construct the set $\Im_{L_m \setminus L_{m-1}}$ by evaluating, using relation (12), an estimate of the reconstruction $F(\mathbf{x}_i)$ for each point $\mathbf{x}_i$ in $L_m \setminus L_{m-1}$, that is:

$$F(\mathbf{x}_i) = \sum_{k \in N_{\mathbf{x}_i}} \overline{W_k}(\mathbf{x}_i) R_k(\mathbf{x}_i), \quad \mathbf{x}_i \in L_m \setminus L_{m-1} \tag{16}$$

  where $N_{\mathbf{x}_i}$ is the set of indexes of the nodes $\mathbf{x}_k \in L_{m-1}$ whose radius of influence contains the point $\mathbf{x}_i$, and $R_k(\mathbf{x})$ are the corresponding nodal functions.
- In the second phase, the data set is enlarged by including the set $(L_m \setminus L_{m-1}, \Im_{L_m \setminus L_{m-1}})$.
- Then, for each point $\mathbf{x}_k \in L_m \setminus L_{m-1}$, the new nodal function $R_k(\mathbf{x})$ is computed by solving the corresponding local interpolation problem.

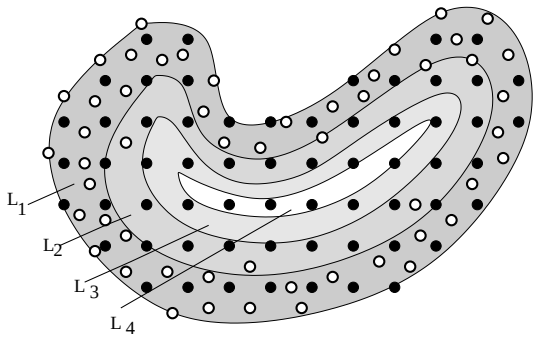

Fig. 1. *Scheme of the layer structure; the white dots represent points in B, while the black are points in G.*

After the processing of all the layers the original data set has been completed, thus allowing us for the evaluation of the reconstruction everywhere.
Determining the layer points represents a critical aspect to the success of the method. As previous mentioned, the local nature of our method allows us to deal always with small sets X_k for each $\mathbf{x}_k \in B$, characterized by a predefined separation distance q_{X_k}, and a fill distance h_{X_k} of the same order of magnitudo. In order to maintain these good properties also for the new points in the layers, the set G has been built with the following grid data density:

$$H_G := \min_{\mathbf{x}_k \in B} h_{X_k}.$$

Then the subdivision of G into layers is obtained by requiring that each point $\mathbf{x}_k \in G$ is considered into a given layer L_m if there is at least a point in L_{m-1} whose distance from $\mathbf{x}_k$ is less than H_G. This choice, in fact, guarantees that the point is in the radius of influence of some of its neighbours and that the error given by (13) is limited.
The multilayer procedure causes inevitably a propagation of the local interpolation error into the hole region. This is due to the fact that the reconstructed values at each step are not all belonging to the original data set, but they are computed using relation (16) and therefore are affected by a reconstruction error. This error is a convex combination of the errors generated by the local interpolation functions $R_k(\mathbf{x})$. A theoretical study of the propagation of this error is, at first glance, very discouraging. In fact, the upper bound of the difference between the local reconstructions of exact and perturbed data, given in the following proposition, shows that the propagation of the perturbation error can be very large.

Proposition 1 *Let $(\mathbf{x}_i, f_i), \mathbf{x}_i \in X_k, f_i \in \Im$ be a set of interpolation points and $(\mathbf{x}_i, \widehat{f}_i), \mathbf{x}_i \in X_k, f_i \in \widehat{\Im}$ the associated perturbed data set. Using relation (10), the error on the local interpolation function $\widehat{R}_k(\mathbf{x})$, is bounded by:*

$$|R_k(\mathbf{x}) - \widehat{R}_k(\mathbf{x})| \leq \|A^{-1}_{X,\varphi}\|_\infty \sum_{i \in I_k} |\varphi(\|\mathbf{x} - \mathbf{x}_i\|_2)| \, \|\mathbf{f}_k - \widehat{\mathbf{f}}_k\|_\infty \tag{17}$$

Proof

$$\begin{aligned} |R_k(\mathbf{x}) - \widehat{R}_k(\mathbf{x})| &\leq \textstyle\sum_{i \in I_k} |c_i - \widehat{c}_i||\varphi(\|\mathbf{x} - \mathbf{x}_i\|_2)| \\ &\leq \max_{i \in I_k}(c_i - \widehat{c}_i) \textstyle\sum_{i \in I_k} |\varphi(\|\mathbf{x} - \mathbf{x}_i\|_2)| = \\ &= \|\mathbf{c} - \widehat{\mathbf{c}}\|_\infty \textstyle\sum_{i \in I_k} |\varphi(\|\mathbf{x} - \mathbf{x}_i\|_2)| \end{aligned}$$

The result follows replacing relation (3). □

This theoretical result suggests that, in order to limit the growth factor in relation (17) ($\|A^{-1}_{X,\varphi}\|_\infty \sum_{i\in I_k} |\varphi(\|\mathbf{x} - \mathbf{x}_i\|_2)|$), the selection of the radial basis functions and of the dimension of the local interpolation problems is really crucial. In our work we are able to maintain a limited growth factor by keeping the system dimension as small as possible, and acting on the inverse multiquadrics constant and on the support of the compactly supported RBF. Moreover this allows us to have a good local control on the shape reconstruction.
Our experimental results support our choices revealing a limited error in the reconstruction of test data sets (see section 6) and obtaining a plausible reconstruction by expanding the shape of the boundary data.
In the next section, an efficient hole filling procedure which implements the multilayers method has been integrated in the basic reconstruction algorithm in order to manage any number of holes.

5 The reconstruction algorithm with hole filling

The basic algorithm for the reconstruction of a surface $F(\mathbf{x})$, starting from a set $(X, \Im)$ of $N = |X|$ distinct points, consists of a preprocessing and two main phases. In the preprocessing the data X are scaled in $[0,1] \times [0,1]$, and they are suitably organized and stored in a grid data structure. Following [9], we used a uniform 2D grid of cells as efficient data structure, which allowed us to design a fast procedure for performing a nearest-neighbour search. Algorithm 1 describes the main steps of our approach.

Algorithm 1 (Surface Reconstruction)
INPUT: $(X, \Im), N_q, N_W, q, \varphi$
OUTPUT: $F(\boldsymbol{\xi}), \quad \boldsymbol{\xi} \in \bar{\Omega}$

COEFFICIENT PHASE: Compute the coefficients of the local interpolant $R_k(\mathbf{x}), k = 1, \cdots, N$

for each $\mathbf{x}_k \in X$,

Construct a set I_k *of* N_q *indexes s.t.* $X_k = \{\mathbf{x}_k\} \cup \{\mathbf{x}_j \in X; \mathbf{x}_j \in Neigh(\mathbf{x}_k)\} \quad and \quad q_{X_k} \geq q$

Compute the radius of influence r_{W_k} *of* $\mathbf{x}_k$ *using* N_W *points;*

Interpolation step:

Build the matrix $A_{X_k,\varphi} \in \mathbb{R}^{N_q \times N_q}$, $A_{X_k,\varphi} = \varphi(\|\mathbf{x}_i - \mathbf{x}_j\|_2) \quad i, j \in I_k$

Solve the linear system: $A_{X_k,\varphi}\mathbf{c} = \mathbf{f}_k$

endfor

EVALUATION PHASE: Evaluate the reconstructed surface

for each evaluation point $\boldsymbol{\xi} \in \bar{\Omega}$*:*

Construct a set N_ξ *of indexes of all the nodes* $\mathbf{x}_k$ *s.t.* $\|\boldsymbol{\xi} - \mathbf{x}_k\|_2 < r_{W_k}$

Evaluate $R_k(\boldsymbol{\xi}), \forall k \in N_\xi$ *using (10)*

Compute the weight $\overline{W_k}(\boldsymbol{\xi})$ *,* $\forall k \in N_\xi$*, using (11) with* $p = 2$

Compute $F(\boldsymbol{\xi}) = \sum_{k\in N_\xi} \overline{W_k}(\boldsymbol{\xi}) R_k(\boldsymbol{\xi})$

endfor

In the first phase (*COEFFICIENT PHASE*) the most important step is the construction of the sets $X_k \subset X$, as already underlined in the previous section. For this aim, we look for $N_q - 1$ points in the area around $\mathbf{x}_k$ ($Neigh(\mathbf{x}_k)$), such that the separation distance of X_k is greater than a given constant q. From an implementation point of view, this means selecting the corresponding set of indexes I_k. In our implementation, q is the same for each X_k.
Then we compute the influence radii r_{W_k} of $\mathbf{x}_k$, chosen large enough to include N_W points of X. Finally, in order to compute the coefficients of the nodal functions $R_k(\mathbf{x})$, we solve

the linear system $A_{X_k,\varphi}\mathbf{c} = \mathbf{f}_k$, where the elements of $\mathbf{f}_k$ are the function values corresponding to the nodes in X_k. The coefficient matrix $A_{X_k,\varphi}$ is symmetric and positive definite. Thus the linear system is solved by applying a Cholesky factorization.
The second phase (*EVALUATION PHASE*) provides the values of the reconstructed function F on a set of points $\bar{\Omega} \subset \mathbb{R}^2$. For each evaluation point $\boldsymbol{\xi}$ the algorithm detects the set N_ξ of indexes of all the nodes $\mathbf{x}_k$, whose radii of influence r_{W_k} include $\boldsymbol{\xi}$, and it computes the local contributions (10) in $\boldsymbol{\xi}$. Thus the reconstructed surface $F(\boldsymbol{\xi})$ is evaluated by weighting all the nodal functions according to (12). In order to obtain a reconstructed surface using the least square criterion, a new input parameter N_c is required, which indicates the number of centers to consider for the computation of the local approximant $R_k(\mathbf{x})$. In this case we construct the set $S_k \subset X_k$ given by $\mathbf{x}_k$ and its $N_c - 1$ suitable neighbours. This subset S_k can be chosen in several way as, for example, using the farthest star-spread neighbours of x_k. We then compute the coefficients of the nodal function $R_k(\mathbf{x})$ by solving the overdetermined linear system $B_{X_k,\varphi}\mathbf{c} = \mathbf{f}_k$ using a QR algorithm. Therefore, we follow Algorithm 1, in which the interpolation step is replaced with:

Approximation step:

Construct the set J_k of $N_c(\leq N_q)$ indexes of points $\in S_k$

Build the matrix $B_{X_k,\varphi} \in \mathbb{R}^{N_q \times N_c}$, $B_{X_k,\varphi} = \varphi(\|\mathbf{x}_i - \mathbf{x}_j\|_2) \quad i \in I_k, j \in J_k$

Solve the overdetermined linear system: $B_{X_k,\varphi}\mathbf{c} = \mathbf{f}_k$

Note that, in the evaluation phase, the local approximant $R_k(\mathbf{x})$ is given by (15) instead of (10).
Now, following Section 4, we extend the previous reconstruction algorithm (Algorithm 1) by completing it with an efficient hole filling procedure (named Algorithm 2). This has been designed to be able to manage topological complex holes and restore surface shapes, preserving the geometry where it exists, while producing smooth transitions to plausible geometry in unobserved areas.

Algorithm 2 (Surface Reconstruction with hole filling)
INPUT: $(X, \Im), N_q, N_W, q, \varphi, B_i, i = 1, \cdots, n_H$
OUTPUT: $F(\boldsymbol{\xi}), \quad \boldsymbol{\xi} \in \bar{\Omega}$

PRELIMINARY PHASE
for each marked hole $i = 1, \cdots, n_H$
Overlap a grid of points G_i on B_i;
Label points in G_i in NL_i layers, s.t. $B_i = L_0 \subset L_1 \subset L_2 \subset \cdots \subset L_{NL_i} \equiv G_i \cup B_i$;
endfor
COEFFICIENT PHASE: *for the set X*
HOLE FILLING PHASE:
for each marked hole B_i $i = 1, \cdots, n_H$
for each layer $L_\ell, \quad \ell = 1, \cdots, NL_i$
EVALUATION PHASE: *compute* $\{\Im_{L_\ell \setminus L_{\ell-1}}\}$
$X = X \cup \{L_\ell \setminus L_{\ell-1}\}; \quad \Im = \Im \cup \{\Im_{L_\ell \setminus L_{\ell-1}}\};$
COEFFICIENT PHASE: *compute* $R_k(\mathbf{x})$ *for* $\mathbf{x}_k \in \{L_\ell \setminus L_{\ell-1}\}$
endfor
endfor
EVALUATION PHASE: *for the set* $\bar{\Omega}$

The critical aspect of Algorithm 1 and Algorithm 2 turns out to be the choice of the free parameters, namely N_q, N_W and q, which influences both the reconstruction quality and the computational complexity. For the right values of these free parameters we have followed the guidelines given in the theoretical analysis of Section 2.
Concerning the computational complexity of these algorithms, this is due both to the numerical computation and to the data structure management. The former can be well quantified in the solution of N linear systems of dimension N_q (interpolation case) using Cholesky factorization, i.e. a computational cost of $O(N \cdot \frac{N_q^3}{6})$ for the coefficient phase, and in the evaluation of the reconstruction in a generic point $\boldsymbol{\xi}$, whose cost is $O(N_q \cdot M)$, where $M = |N_\xi|$.
Regarding the spatial data structure, we can clearly single out a building cost in the preprocessing phase of $O(N)$, while the complexity of any search inside the fixed grid depends on the number of cells visited, and therefore on the separation distance q, on the density h and, of course, on the number of searched points N_q for each linear system.

6 Numerical Results

The surface reconstruction algorithm described in this work has been implemented and tested with several range images acquired with a PICZA PIX-30 touching probe scanner (Dep. of Math., University of Bologna), and with a VIVID 900 laser scanner (ENEA, Bologna). The scanning technologies considered acquire the shape of an object by generating regular range images. However, since they present outliers and systematic range distorsions, they can be considered quasi-uniform data sets.

Fig. 2. *Reconstructed* angel *data set using Algorithm 1.*

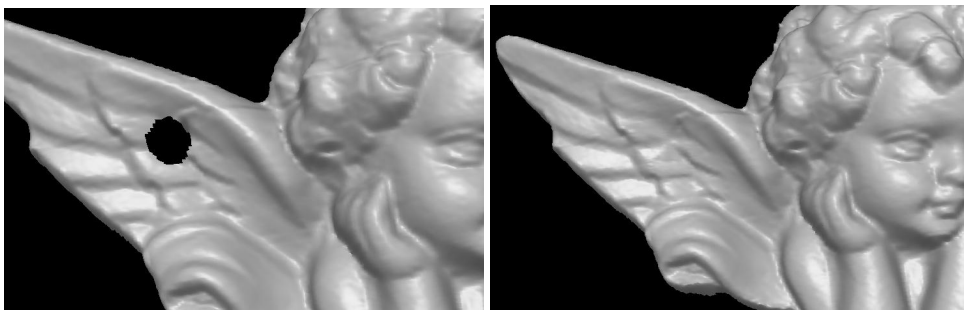

Fig. 3. *Reconstructed* angel-h1 *data set: (left) Algorithm 1; (right) Algorithm 2*

To illustrate the behaviour of our algorithm, we have reported the results from two data sets.

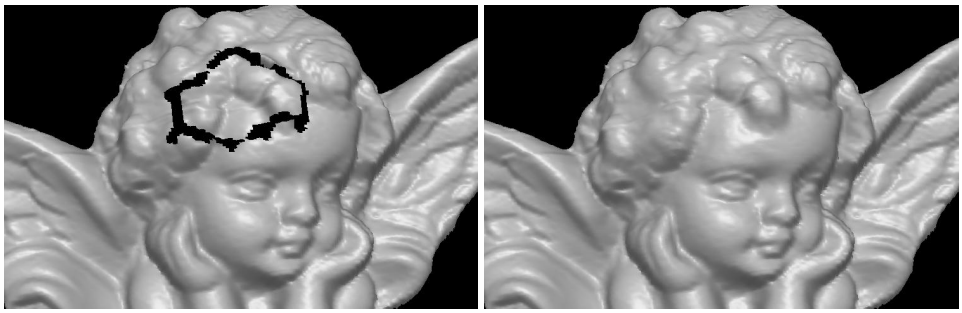

Fig. 4. *Reconstructed* angel-h2 *data set: (left) Algorithm 1; (right) Algorithm 2*

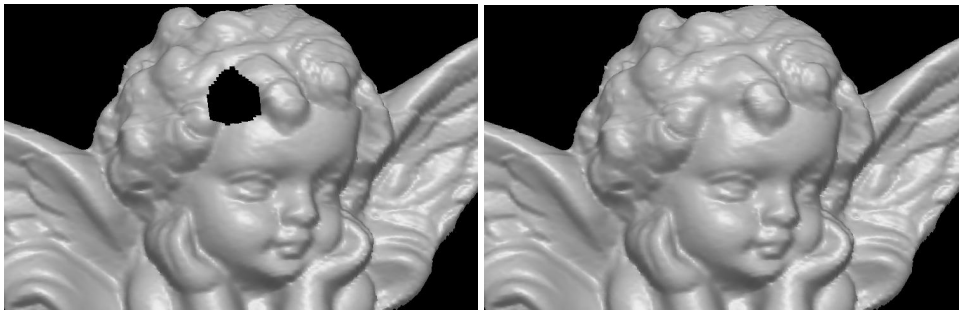

Fig. 5. *Reconstructed* angel-h3 *data set: (left) using Algorithm 1; (right) using Algorithm 2*

The first data set (*angel*) has been acquired using PICZA scanner and it does not present any holes. This has been used both to test reconstruction Algorithm 1 and to verify the quality of the hole filling procedure. For this purpose we have removed parts of the data in different regions to create synthetic holes (*angel-h1*,*angel-h2* and *angel-h3*) with different topologies. All the regions considered are characterized by convoluted details, because it is well known that, for simple and relatively flat holes, the reconstruction by radial basis functions naturally works pretty well [2].
The second data set (*minerva*) presents two holes due to the scanner acquisition, one in the neck and the other under the nose. Moreover, a vertical data zone has intentionally been removed in order to simulate a restoration by hiding the join between the two parts of the statue, while this join has been left on the lips and chin. This data set has been acquired by a VIVID laser scanner and presents inherent noise due to the laser scanner acquisition.
The examples have been obtained using the inverse multiquadric radial basis functions, and similar results have been produced by Wendland's compact support radial basis functions. For each local interpolant/approximant on X_k the constant γ_k of the inverse multiquadric functions and the support α_k of the Wendland's basis functions, have been automatically adapted to be proportional to the support of the local problems according to the formula: $const \cdot \max_{x_i \in X_k} \|x_k - x_i\|_2$.
This yields a common reproducing quality for all the nodal functions $R_k(\mathbf{x})$ and therefore a better quality for the global interpolant/approximant. In our examples, where the data are scaled in $[0,1] \times [0,1]$, the constant $const$ has been chosen to be 0.35.
Fig.2 shows the reconstruction of the *angel* data set obtained with Algorithm 1, using the interpolation criterion. Algorithm 1 has also been applied to the incomplete *angel* data sets, highlighting the algorithm's ability to preserve a hole in the data sets when desired. The results of these reconstructions are displayed in Fig.3(left), Fig.4(left) and Fig.5(left). The corresponding reconstruction, obtained using the hole filling procedure (Algorithm 2), are given in Fig.3(right), Fig.4(right) and Fig.5(right). The quality of these reconstructions can be appreciated by comparing them with the reconstructions of the complete data set (Fig.2)

DATA SET	No.Points	N_W	N_q	H_X	q	T_c	T_e	T_{TOT}
angel	13956	9	9	$1.5e^{-3}$	$0.5e^{-3}$	4.34	1.86	6.36
minerva	17050	9	9	$1.8e^{-3}$	$0.5e^{-3}$	6.19	1.89	8.28

Table 1
Computational results (in seconds) of Algorithm 1.

DATA SET	No.Points	N_W	N_q	H_X	q	T_c	T_{hf}	T_e	T_{TOT}
angel-h1	13856	9	9	$1.5e^{-3}$	$0.5e^{-3}$	4.30	2.78	2.06	9.34
angel-h2	13583	9	9	$1.5e^{-3}$	$0.5e^{-3}$	4.19	11.08	2.56	18.11
angel-h3	13783	9	9	$1.5e^{-3}$	$0.5e^{-3}$	4.27	5.90	2.25	12.63
minerva (int)	17050	9	9	$1.8e^{-3}$	$0.5e^{-3}$	6.18	12.16	5.00	23.66
minerva (app)	17050	20	20	$1.8e^{-3}$	$0.5e^{-3}$	8.17	14.05	5.02	27.23

Table 2
Computational results (in seconds) of Algorithm 2.

and the corresponding reconstruction errors have always been below 5%.

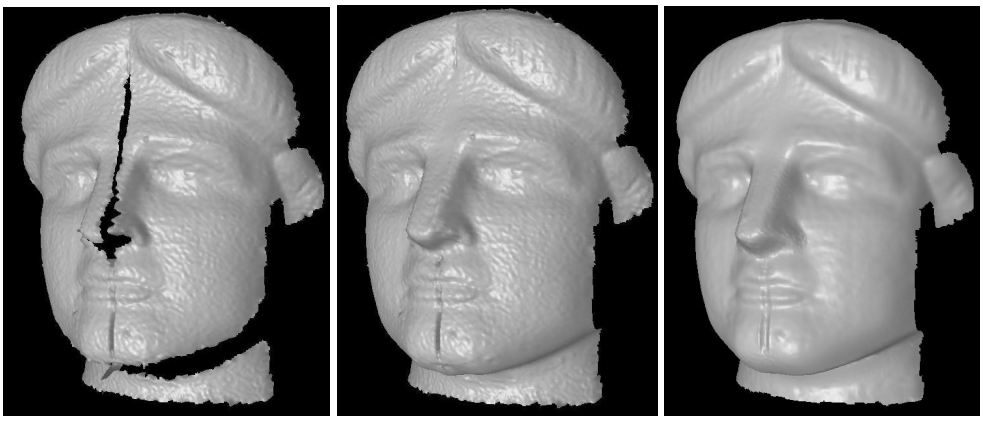

Fig. 6. *Reconstructed* minerva *data set: (left) Alg. 1; (center) Alg. 2 (int.); (right) Alg. 2 (app.)*

Similarly, we applied Algorithm 1 to the *minerva* data set using the interpolation procedure to preserve the inherent noise and the holes of the original data (Fig.6(left)). The surface obtained using Algorithm 2 with interpolation is shown in Fig.6(center), while Fig.6(right) is an example of removing the noise in the reconstruction using the approximation procedure. Obviously the amount of smoothing applied can easily be modified, considering different choices for the number of centers (N_c) and the number of points used in the local approximation (N_q). Note that in Fig.6(right) we used $N_c = 6$ and $N_q = 20$. The illustrations show the high quality of the reconstruction.

Another key aspect of the proposed algorithms is their efficiency, due to the local nature of the method. Tables 1 and 2 quantify the computational time of the main phases of Algorithm 1 and 2, respectively, running on a PC Intel Pentium IV, 2.4GHz, with 1Gb of RAM. In the T_{TOT} column we report the execution time of the algorithms, including the preprocessing phase, while the T_c, T_{hf} and T_e report the computational time of the coefficient, the hole filling and the evaluation phases, respectively. The latter strongly depends on the evaluation grid used; all the reconstructed surfaces we considered have been evaluated in a 300×300 uniform grid.

In the tables we also report the free parameters N_W, N_q, the separation distance q and the estimated density H_X of the data sets. Note that the latter corresponds to the acquisi-

tion step of the scanner and its value represents the fill distance of the local interpolation problems and it has been used to estimate the separation distance q. This has allowed us to satisfy the quasi-uniformity conditions (8), guaranteeing a compromise between stability and quality. In fact, the uniformity parameter ρ of the sets X_k turns out to be $\rho \leq 0.67$ for the *angel* data set and $\rho \leq 0.55$ for the *minerva* data set. Note that, in the *minerva* data set, we could have considered a slightly bigger value for q yielding a bigger density value, but the algorithm would have been less efficient.

Acknowledgements This work has been supported by MIUR-Cofin 2002. We are grateful to Ing. S. Petronilli (ENEA, Bologna) for providing the data and motivation for this research. We also thank the referees for many useful comments.

References

[1] Bajaj, C.L., Bernardini F., Xu G., Automatic reconstruction of surfaces and scalar fields from 3D scans *in Proc. of SIGGRAPH 1995, ACM Press*, (1995).

[2] Carr, J.C., R.K.Beatson, J.B. Cherrie, T.J.Mitchell, W.R.Fright, B.C.McCallum, T.R. Evans, Reconstruction and representation of 3D objects with radial basis functions, *in Proc. of SIGGRAPH 2001, ACM Press*, (2001) 67–76.

[3] Davis J., Marshner S.R., Garr M., Levoy M., Filling holes in complex surfaces using volumetric diffusion. *Proc. First International Symposium on 3D Data Processing, Visualization, Transmission*, (2001).

[4] Floater, M.S., Iske A., Multistep scattered data interpolation using compactly supported radial basis functions , *Journal of Comput. Appl. Math.* **73(5)**, (1996) 65–78.

[5] Gordon, W.J., Wixson J.A., Shepard's method of metric interpolation to bivariate and multivariate interpolation, *Mathematics of Computation* **32(141)**, (1978) 253–264.

[6] Hoppe, H., DeRose T., Duchamp T., McDonald J., Stuetzle W., Surface Reconstruction from unorganized points, *in Proc. of SIGGRAPH 1992, ACM Press*, (1992).

[7] Lazzaro, D. and Montefusco, L.B., Radial basis functions for the multivariate interpolation of large scattered data sets, *Journal of Computational and Applied Mathematics* **140**, (2002) 521–536.

[8] Madich W.R., Nelson S.A., Bounds on multivariate polynomials and exponential error estimates for multiquadric interpolation. *Journal of Approximation Theory* **70**, (1992) 94–114.

[9] Renka, R.J., Multivariate interpolation of large sets of scattared data, *ACM Trans. Math Software* **14,2**, (1988) 139–148.

[10] Schaback, R., Creating surfaces from scattared data using radial basis functions, *in M.Daehlen, T.Lyche, L. Schumaker (Eds), Mathematical Methods for Curves and Surfaces, Vanderbilt University Press, Nashville*, (1995) 477–496.

[11] Schaback, R., Error estimates and condition numbers for radial basis function interpolation, *Adv. Comput. Math.* **3**, (1995) 251–264.

[12] Wendland, H., Error estimates for interpolation by compactly supported radial basis functions of minimal degree, *Journal of Approximation Theory* **93**, (1998) 258–272.

[13] Wu, Z., Multivariate compactly supported positive definite radial functions, *Adv. Comput. Math.* **4**, (1995) 283–292.

[14] Wendland, H., Piecewise polynomial, positive definite and compactly supported radial functions of minimal degree, *Adv. Comput. Math.* **4**, (1995) 359–396.